Vacancy engineering enhanced photothermal-catalytic properties of Co_9S_{8-x} nanozymes for mild NIR-II hyperthermia-amplified nanocatalytic cancer therapy

Yongyu Hao[a,1], Nan Wang[b,c,1], Jiaxu Wang[a], Shuilin Shao[a], Bo Gao[a], Youping Tao[a], Litao Huo[a], Lang Yan[d], Jigong Wu[a,*], Zhiming Chen[a,*]

[a] Department of spine surgery, the ninth Medical Center of PLA General Hospital, Beijing 100101, China

[b] Department of Obstetrics and Gynecology, the First Medical Center, Chinese PLA General Hospital, Beijing 100853, China

[c] Medicine School of Chinese PLA, Beijing 100853, China

[d] Department of Health Toxicology, Faculty of Naval Medicine, Naval Medical University, Shanghai, 200433, China

* Corresponding authors.

E-mail addresses: docwjg@126.com (J. Wu); czm306@163.com (Z. Chen)

[1] These authors contributed equally to this work.

Fig. S1 Photographs of Co_9S_{8-x} dispersed in DI water, FBS, or DMEM for different times.

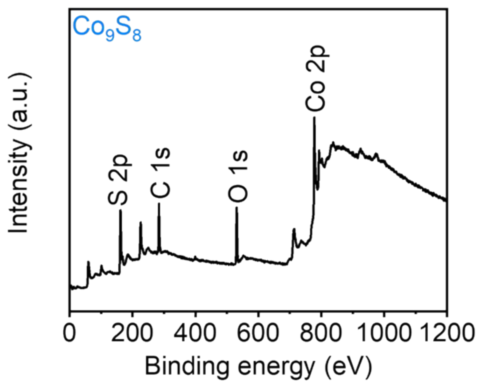

Fig. S2 Survey XPS spectrum of Co_9S_8.

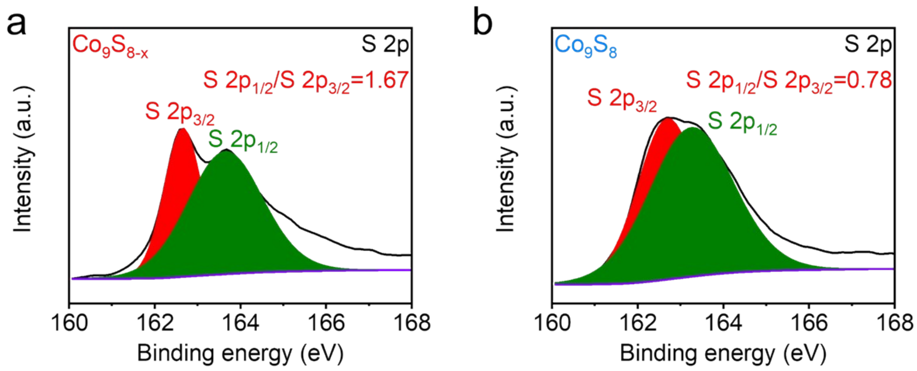

Fig. S3 High-resolution S 2p spectrum of Co_9S_{8-x} and Co_9S_8.

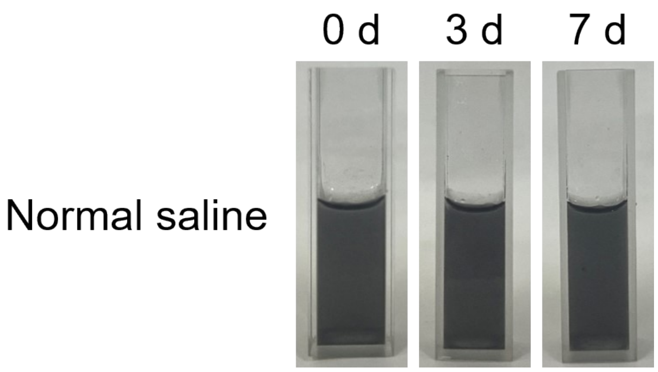

Fig. S4 Photographs of Co_9S_{8-x} storing in normal saline for different times.

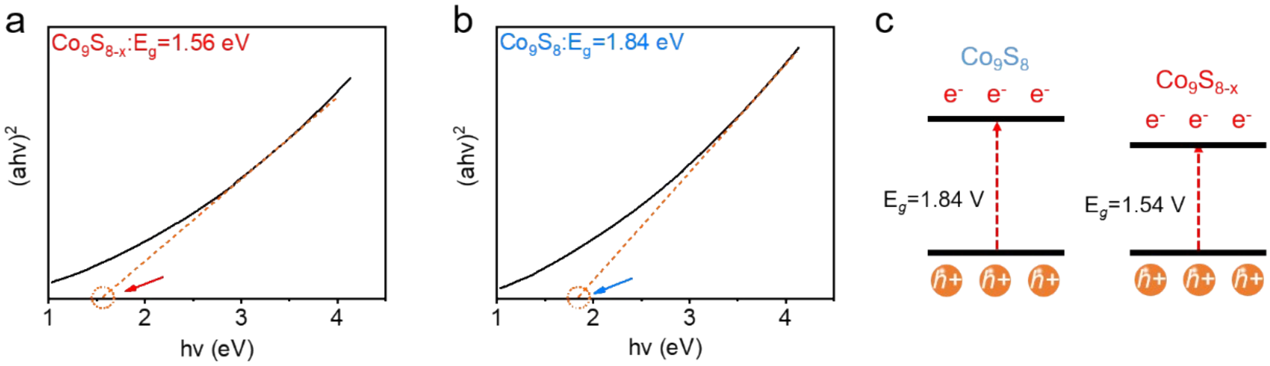

Fig. S5 (a, b) Bandgap of Co_9S_{8-x} and Co_9S_8. (c) Scheme of the decreased bandgap structures of Co_9S_{8-x} induced by V_S-doping.

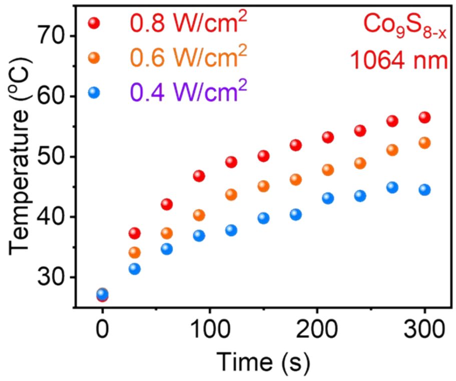

Fig. S6 NIR-II photothermal properties measurements of Co_9S_{8-x}.

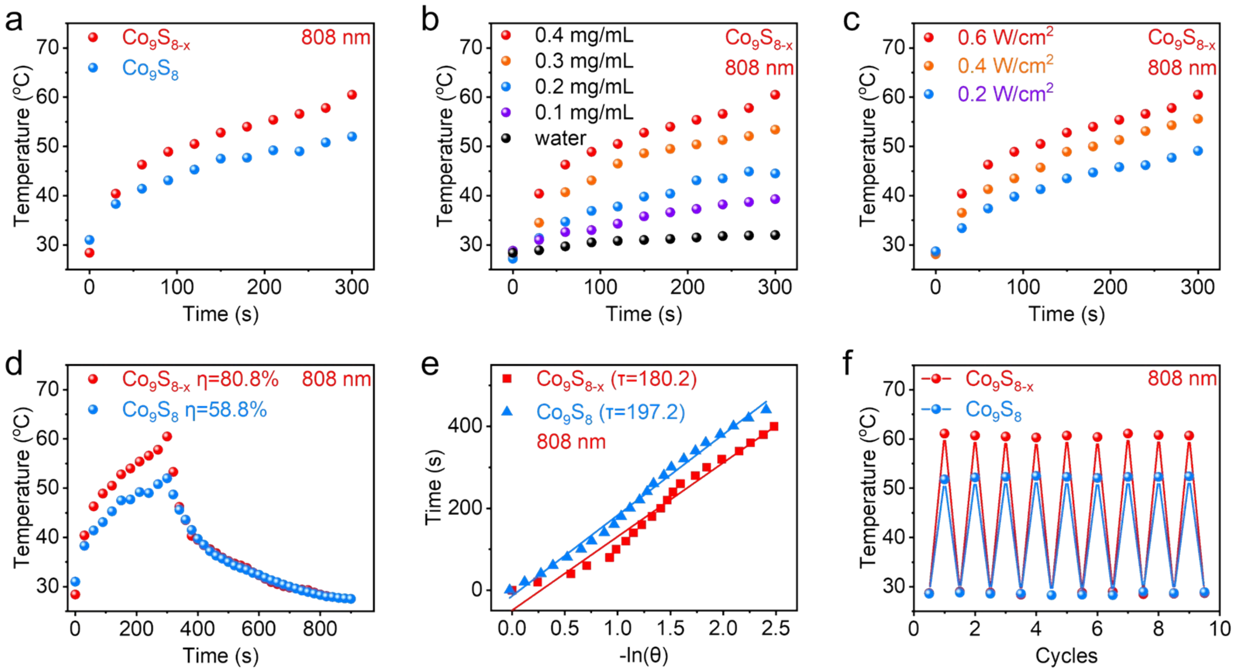

Fig. S7 NIR-I photothermal properties measurements including concentration-dependent behaviors, stability, conversion efficiency, and infrared thermal images of Co_9S_{8-x}.

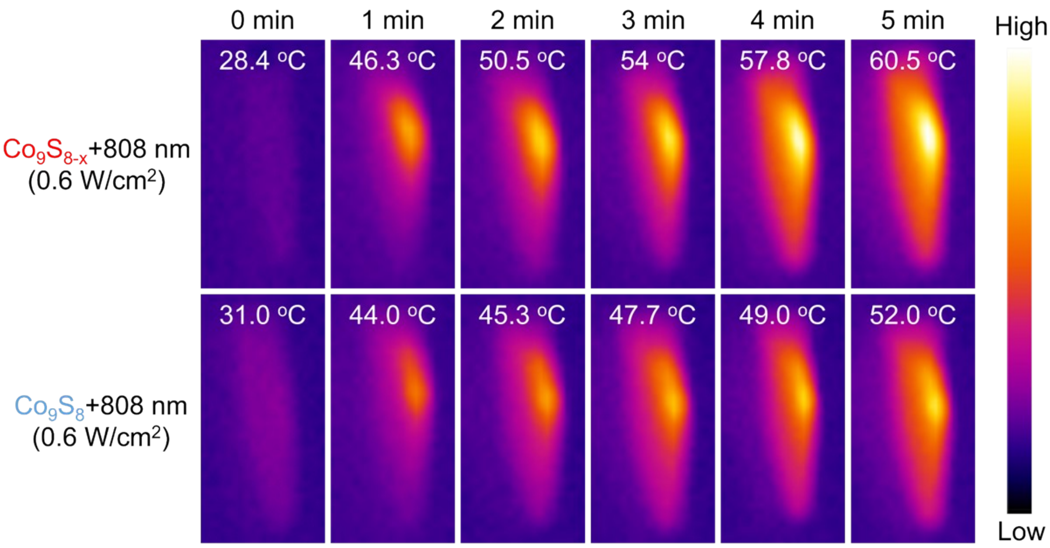

Fig. S8 Infrared thermal images of Co_9S_{8-x} and Co_9S_8 under 808 nm laser irradiation.

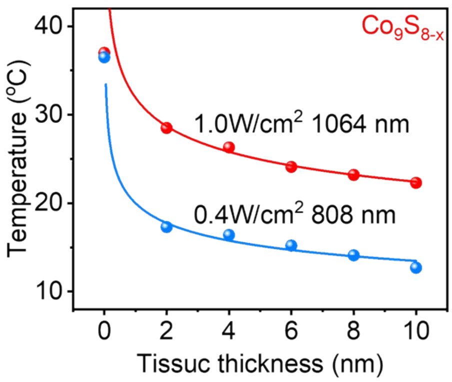

Fig. S9 Deep tissue photothermal property evaluation of Co_9S_{8-x} in the presence of additional chicken breast tissues at varied thickness.

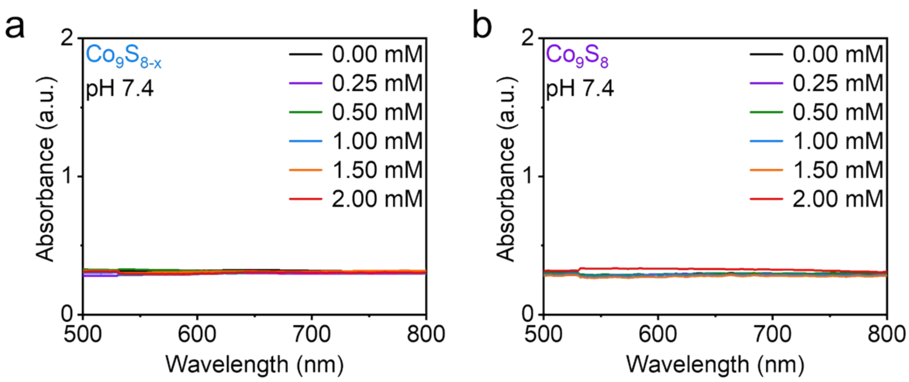

Fig. S10 Evaluation of POD-mimic catalytic activity of Co_9S_{8-x} and Co_9S_8 in the presence of H_2O_2 at pH 7.4.

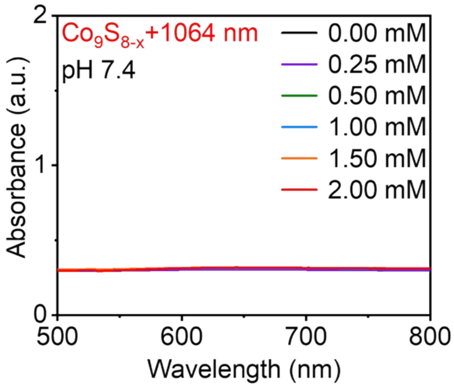

Fig. S11 Evaluation of POD-mimic catalytic activity of Co_9S_{8-x} + 1064 in the presence of H_2O_2 at pH 7.4

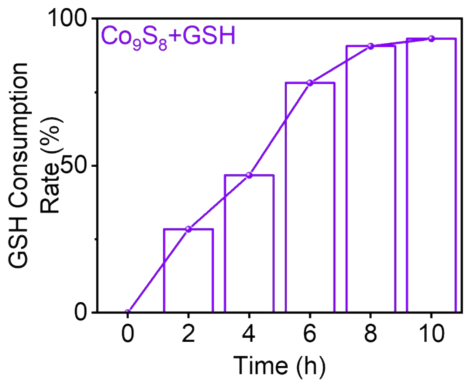

Fig. S12 Evaluation of GSH-px-mimic catalytic activity of Co_9S_{8-x}.

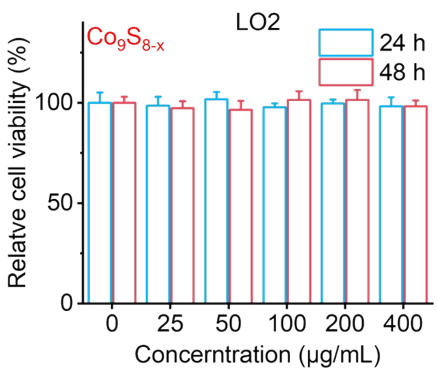

Fig. S13 Relative cell viabilities of LO2 cells incubated with Co_9S_{8-x} with varied concentrations for 24 or 48 h.

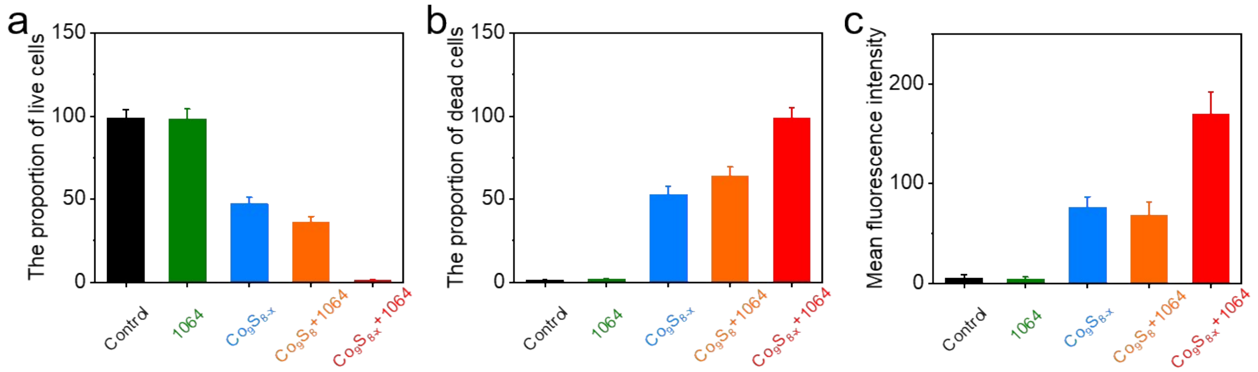

Fig. S14 (a, b) Semi-quantitative analysis of live/dead cell staining and ROS staining determined by the Image J software. Data are presented as mean values ± SD (n = 3).

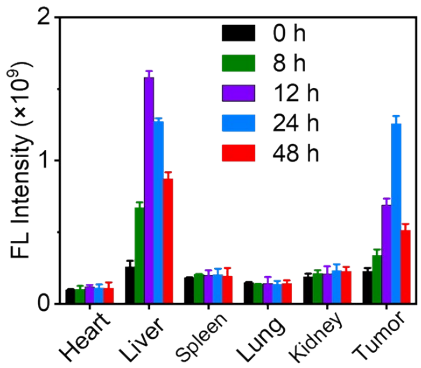

Fig. S15 Time-dependent fluorescence intensity of Co_9S_{8-x} in the major organs and tumor tissues.

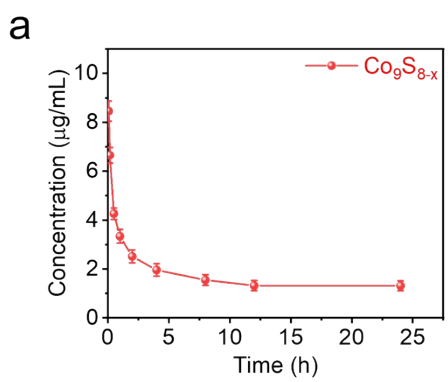

b

Parameters	Co_9S_{8-x}
C_{max} (μg/mL)	8.8±0.3
$t_{1/2}$ (h)	8.4±0.8
$AUC_{(o-\infty)}$ (μL•h/mL)	49.7±6.8
$MRT_{(o-\infty)}$ (h)	14.6±1.4
CL (L/h/kg)	0.03±0.008

Fig. S16 Plasma concentration-time profiles (a) and pharmacokinetic parameters (b) of Co_9S_{8-x} after intravenous administration (n = 5).

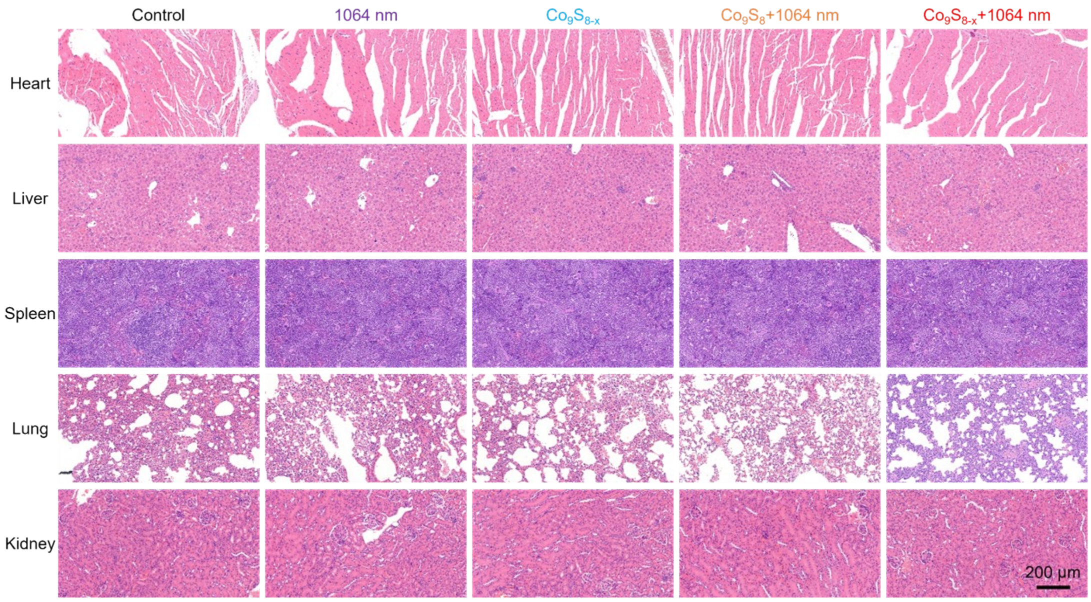

Fig. S17 H&E-stained images obtained from the major organs (heart, liver, spleen, lung, and kidney) of mice in different treatment groups.

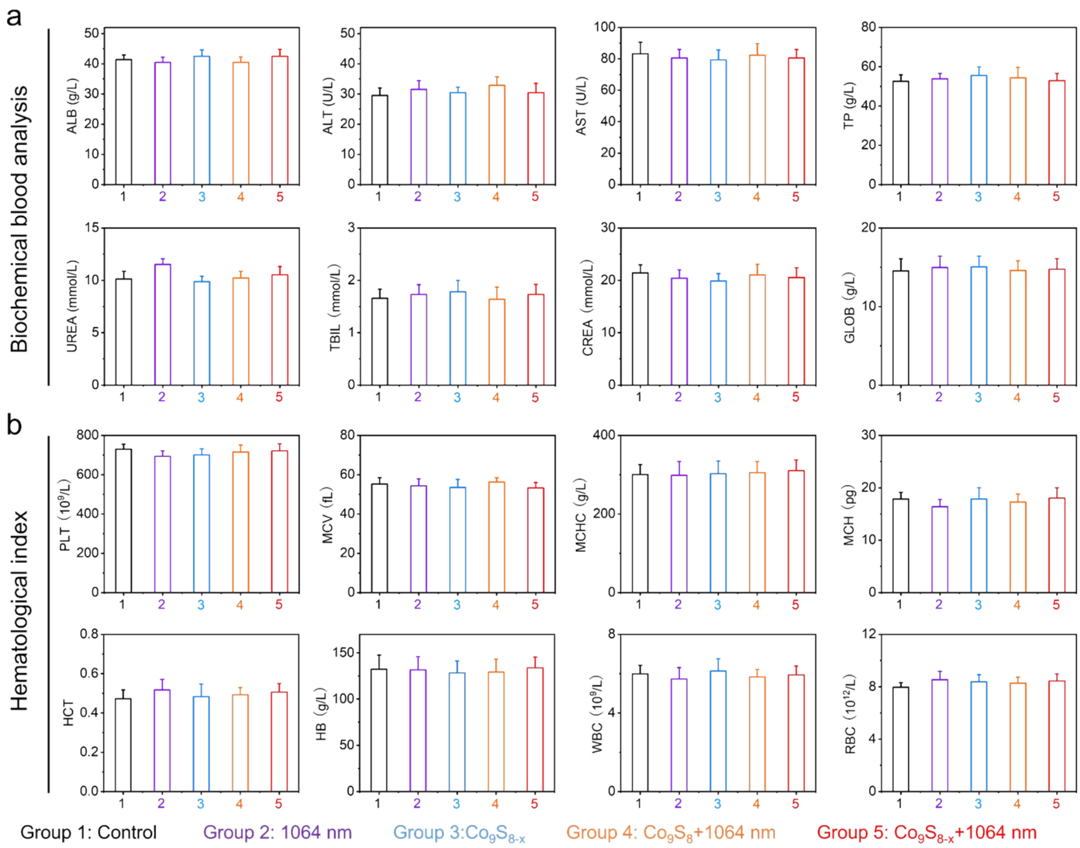

Fig. S18 (a-b) Biochemical blood analysis (a) and hematological index (b) of the mice that were sacrificed at 18 days after different treatments. The terms of biochemical blood analysis include ALB, ALT, AST, TP, UREA, TBIL, CREA, and GLOB. The terms of hematological index include PLT, MCV, MCHC, MCH, HCT, Hb, WBC, and RBC.

Table S1. Comparison of the photothermal conversion efficiency of Co_9S_{8-x} with other previously reported PTT agents.

PTT agents	Photothermal conversion efficiency	Laser	References
Co_9S_{8-x}	53.4%	1064 nm	This work
$Bi_{2-x}Mn_xO_3$	52.31%	808 nm	1
PDA@POM	40.9%	808 nm	2
PB NPs	47.01%	808 nm	3
MG 1655-M	42.3%	808 nm	4
$Bi_{19}S_{27}I_3$	41.5%	1064 nm	5
BP	28.4%	1064 nm	6
$SiO_x/CeO_2/VO_x$	20.01%	1064 nm	7
Au NPs	24.1%	1064 nm	8
BCPH NSs	47.8%	1064 nm	9
$Ce\text{-}MoO_{v3}$	49.86%	1064 nm	10

Table S2. Comparison of the POD-like catalytic activity of Co_9S_{8-x} with other previously reported nanozymes.

Nanozymes	$\boldsymbol{V_{max}}$	$\boldsymbol{K_m}$	**pH**	**References**
Co_9S_{8-x}	0.9×10^{-7} M s^{-1}	6.4 mM	5.0	This work
COF@Co_3O_4	2.3×10^{-8} M s^{-1}	2.1 mM	6.5	11
Ru/TiO_{2-x}@TiCN	1.4×10^{-8} M s^{-1}	0.23 mM	6.5	12
LDH-250	4×10^{-8} M s^{-1}	0.24 mM	6.5	13
FePd-TPP/ADM	1.69×10^{-9} M s^{-1}	3.65 mM	4.0	14
A-Gel-GOx-Fc	2.32×10^{-9} M s^{-1}	7.6 mM	6.0	15
PEG/Cu-COF	2.52×10^{-8} M s^{-1}	0.96 mM	4.5	16

References

1. X. Ma, B. Chen, H. Wu, Q. Jin, W. Wang, Z. Zha, H. Qian, Y. Ma, *J. Mater. Chem. B*, 2022, **10**(18), 3452-3461.
2. Q. Meng, W. Wang, H. Wang, Y. Tao, N. Anastassova, T. Sun, Y. Sun, L. Wang, *J. Colloid. Interf. Sci.*, 2022, **678**, 796-803.
3. H. Pang, C. Tian, G. He, D. Zhang, J. Yang, Q. Zhang, R. Liu, *Nanoscale*, 2021, **13**(18), 8490-8497.
4. W. Song, Y. He, Y. Feng, Y. Wang, X. Li, Y. Wu, S. Zhang, L. Zhong, F. Yan, and L. Sun, *Small*, 2024, **20**(26), 2305764.
5. J. Xiong, Q. Bian, S. Lei, Y. Deng, K. Zhao, S. Sun, Q. Fu, Y. Xiao, B. Cheng, *Nanoscale*, 2021,

13(10), 5369-5382.

6. B. Geng, W. Shen, P. Li, F. Fang, H. Qin, X. Li, D. Pan, L. Shen, *ACS Appl. Mater. Interfaces*, 2019, **11**(48), 44949-44960.
7. R. Zhao, R. Zhang, L. Feng, Y. Dong, J. Zhou, S. Qu, S. Gai, D. Yang, H. Ding, P. Yang, *Nanoscale*, 2022, **14**(2), 361–372.
8. L. Sun, Y. Chen, F. Gong, Q. Dang, G. Xiang, L. Cheng, F. Liao, M. Shao, *J. Mater. Chem. B*, 2019, **7**(28), 4393-4401.
9. C. Chen, W. Zhang, Y. Ouyang, Y. Tan, S. Zhao, Y. Chen, L. He, S. Lu, H. Ran, H. Liu, *ACS Appl. Nano Mater.*, 2023, **6**(9), 7572-7581.
10. S. Wen, Y. Shi, Y. Zhang, Q. Chang, H. Hu, X. Deng, Y. Xie, *Langmuir*, 2023, **39**(29), 10145-10153.
11. C. Feng, J. Hu, C. Xiao, J. Yang, B. Xin, Z. Jia, S. Zhang, G. Tian, D. Zhang, L. Geng, L. Yan, L. Wang, B. Geng, *Chem. Eng. J.*, 2023, **460**, 141874.
12. Y. Zhao, B. Yuan, L. Yan, Z. Wang, Z. Xu, B. Geng, X. Guo, X. Chen, *Adv. Sci.*, 2024, **11**(4), 2307029.
13. R. Xu, D. Zhang, S. Chen, J. Qiu, X. Liu, *Appl. Clay. Sci.*, 2023, **239**, 106949.
14. W. Xie, G. Zhang, Z. Guo, J. Lu, J. Ye, W. Xu, X. Gao, K. Yue, Y. Wei, L. Zhao, *Adv. Funct. Mater.*, 2022, **32**(12), 2107518.
15. Y. Zhao, J. Du, Z. Xu, L. Wang, L. Ma, L. Sun, *Adv. Sci.*, 2024, **11**(10), 2308229.
16. X. Zhu, T. Feng, Y. Chen, Y. Xiao, W. We, X. Zhang, D. Wang, S. Wang, J. Liang, H. Xiong, *Chem. Eng. J.*, 2024, **488**, 150770.